Bulletin of Atmospheric Science and Technology (2021) 2:2
https://doi.org/10.1007/s42865-021-00031-y

RESEARCH ARTICLE

Changes in precipitation and evapotranspiration over Lokok and Lokere catchments in Uganda

Ambrose Mubialiwo [1,2] · Cyrus Chelangat [1] · Charles Onyutha [2]

Received: 7 October 2020 / Accepted: 17 February 2021/Published online: 24 March 2021

Abstract

This study analysed long-term (1948–2016) changes in gridded (0.25° × 0.25°) Princeton Global Forcing (PGF) precipitation and potential evapotranspiration (PET) data over Lokok and Lokere catchments. PGF-based and station datasets were compared. Trend and variability were analysed using a nonparametric technique based on the cumulative sum of the difference between exceedance and non-exceedance counts of data. Seasonal (March-April-May (MAM), June-July-August (JJA), September-October-November (SON), December-January-February (DJF)) and annual precipitation exhibited negative trends ($p < 0.05$). Positive anomalies in precipitation occurred in the 1950s as well as in the early 2000s till 2016. Negative anomalies existed between 1960 and 2000. Both seasonal and annual PET mainly exhibited increasing trend with alternating positive and negative anomalies for the entire period, except in the southern region. The H_0 was rejected ($p < 0.05$) for SON PET in the North and South of the study area. The H_0 was rejected ($p < 0.05$) for DJF PET in the North. However, H_0 was not rejected ($p > 0.05$) for MAM, JJA and annual PET. Positive and negative correlations were observed between PGF and station precipitation varying from one location to another. The PGF-based *PET* were lower than the observed PET at Kotido by about 40%. Besides, a close agreement was noticeable between PGF-based and MODIS PET from May to November. This showed the need to improve on the quality of PGF data in reproducing the observed climatic data in areas with low meteorological stations density. Nevertheless, the findings from this study are relevant for planning of predictive adaptation to the effects of climate variability on the water resources management applications. Impacts of human factors and climate change on the hydrology of the study area should be quantified in future research studies.

Keywords Trend and variability · Precipitation · Evapotranspiration · Lokok and Lokere catchments

✉ Ambrose Mubialiwo
mambroze@gmail.com

Extended author information available on the last page of the article

1 Introduction

Because of the importance of precipitation and evapotranspiration for agriculture (both crop and livestock) especially in arid and semi-arid climatic zones, assessing the influence of climate variability on these climate variables is vital for predictive adaptation. In this line, several studies have been conducted on trends and variability in climatic variables across the world. Examples of such studies were on the changes in historical precipitation in the Black Sea region of Turkey (Cengiz et al., 2020), trend and variability in rainfall and evapotranspiration over Mpologoma catchment in Uganda, East Africa (Mubialiwo et al., 2020), decadal and/or multi-decadal variability in gridded precipitation and potential evapotranspiration (PET) obtained from Cent-Trends and Princeton Global Forcing (PGF), respectively, across the Lake Kyoga Basin (LKB) (Onyutha et al., 2020) and the influence of several meteorological parameters on evapotranspiration in the humid zone of Pakistan (Adnan et al., 2020). Furthermore, Mahmood et al. (2019) examined the climate variability and trend in the most parts of the lake Chad basin, Africa. In Botswana, Byakatonda et al. (2018) analysed the rainfall and temperature time series to detect climatic trends and variability over semi-arid areas. Sun et al. (2019) studied the seasonal and spatial variation of evapotranspiration in the selected Amazon sub-basins. Paca et al. (2019) assessed the spatial distribution of evapotranspiration across the Amazon River Basin. Owoyesigire et al. (2016) studied trends of variability and extremes in rainfall and temperature in the cattle corridor of Uganda.

In the study area of Lokok and Lokere catchments in Uganda, majority of the populations are pastoralists and agro-pastoralists, mainly relying on rainfall for their activities. However, the variability of weather patterns, such as extreme rainfall, result in disastrous floods, followed by prolonged dry spells and extreme hydrological and agricultural drought (Egeru et al., 2014; Haile et al., 2019; Ministry of Water and Environment, 2017), affecting the economic activities in the area. Impacts of weather extremes in the study area are exacerbated by several human activities such as land use change, uncontrolled bush burning, over-grazing, deforestation and artisanal mining activities. These rainfall-induced disasters result in destruction of property such as roads, bridges, gardens and loss of livestock and human lives. Some of the recent dramatic rainfall-induced disasters in the study area include (1) the devastating floods that washed away the Kangole Bridge disconnecting the Teso region from the Karamoja region in June 2018 (Reliefweb, 2018) and (2) the below-average rainfall of March–June, 2019, which resulted in lack of seasonal vegetables and a great decline in agricultural labour demand, causing high deterioration in household returns and food (Reliefweb, 2020a). In October 2020, flooding incidents were caused by the rise of water levels in various areas including Lake Kyoga and Bisina, thereby affecting several districts including Kumi and Katakwi within the study area. These flooding incidents affected 78,719 people (12,332 household) displacing 10,815 people (Reliefweb, 2020b). The report by Oxfam (2016) categorised the Karamoja and Teso regions as one of the most prone areas to drought and floods. The report by United Nations (2008) further categorises Karamoja region as one of most drought regions in Uganda. In the years 2005, 2006 and 2014, severe drought events affected 600,000, 750,000 and 4 million people, respectively (Oxfam, 2016). Similarly, extraordinary floods occurred in 1997, 2007 and 2010 affected 153,500, 718,045 and 350,000 people, respectively. The floods of 1997 resulted in a death toll of 100 people (Oxfam, 2016). The above evidences the susceptibility of the region to floods and drought. Therefore, knowledge of variability in climatic variables such as precipitation is crucial for predictive planning and management of rainfall-induced disasters, together with agricultural and pastoral practices in the study area.

Several studies on variability in precipitation and the allied variables such as temperature and potential evapotranspiration (PET) have been conducted. However, most of the studies were done at coarse or countrywide scale; see for instance, Nsubuga et al. (2014a and b), Mwaura and Okoboi (2014), Onyutha (2016a), Ssentongo et al. (2018), Jury (2018) and Kisembe et al. (2019). Some studies were done at regional and sub-regional scales, e.g. Kansiime et al. (2013) assessed trend and variability in rainfall in the entire eastern Uganda, Egeru et al. (2014) and Egeru et al. (2019) analysed the rainfall and temperature, but their works were confined in the Karamoja sub-region, and Stampone et al. (2011) examined the local spatio-temporal variability in precipitation around Kibale National Park, in the western Uganda. Other studies were conducted at larger water basins, e.g. Nyeko-Ogiramoi et al. (2013), Onyutha and Willems (2015), Alemu et al. (2015), Onyutha (2016b) and Onyutha et al. (2020). Whereas Onyutha et al. (2020) studied changes in precipitation and PET over Kyoga basin where the study area is located, the variability of rainfall within the main drainage sub-basins of Uganda, Lake Kyoga basin included, fluctuates from one location to another (Nsubuga et al., 2014a and b). Therefore, an in-depth exploration of the changes in precipitation and PET for refined results at localised catchment scales (like Lokok and Lokere) is deemed very crucial.

The study by Onyutha and Willems (2017a) established that the fluctuations in the large-scale ocean–atmosphere conditions describe variability in precipitation more appropriately at a regional than small-sized area. Therefore, to provide an insight on the temporal changes in dry and wet conditions, which is a vital aspect to enable the local pastoralists advance their capability to predict the local precipitation and PET, only the trend and spatio-temporal variability analyses were done. The connection of precipitation and PET with the large-scale ocean–atmosphere conditions at the localised scale of Lokok and Lokere catchments was not part of this study.

Due to lack of observed meteorological data over the study area, variability in precipitation and PET can be analysed using several global climatic products. Some of these products include:

- Global Precipitation Climatology Centre (GPCC) (Meyer-Christoffer et al., 2018)
- Climate Research Unit (CRU) Time series version 4.0 (Harris et al., 2020)
- TAMSAT African Rainfall Climatology (Maidment et al., 2014)
- extended TAMSAT (Tarnavsky et al., 2014)
- Global Precipitation Climatology Project (GPCP) (Adler et al., 2018)
- Princeton Global Forcing (PGF) (Sheffield et al., 2006)
- Climate Hazards group Infrared Precipitation with Stations (CHIRPS) (Funk et al., 2015)
- Precipitation Estimation from Remotely Sensed Information using Artificial Neural Networks Climate Data Record (PERSIANN-CDR) (Ashouri et al., 2015)
- Tropical Rainfall Measuring Mission (TRMM), Multi-satellite Precipitation Analysis (TMPA) (Huffman et al., 2007)
- Global Precipitation Measurement mission (GPM) (Merzdorf, 2019)
- African Rainfall Climatology (ARC) (Novella and Thiaw, 2013)

However, most of these products are either of short-term records. The PGF dataset series are of the long-term record length (from 1948 to 2016) and have fine spatial resolution (0.25° × 0.25°). The PGF observational-based dataset was developed using a blend of National Centers for Environmental Prediction–National Center for Atmospheric Research (NCEP-NCAR)

reanalysis dataset (Kalnay et al., 1996) and other several global, observational datasets including the Climate Research Unit (CRU) TS2.0, Tropical Rainfall Measuring Mission (TRMM), Global Precipitation Climatology Project (GPCP) and National Aeronautics and Space Administration (NASA) Langley Surface Radiation Budget (Sheffield et al., 2006). The robustness of the PGF data for trend and variability analyses was demonstrated in several studies (Li et al., 2019; Mubialiwo et al., 2020; Onyutha et al., 2020; Onyutha and Willems, 2017b) in various regions of the world. The high spatial resolution (0.25° × 0.25°) of the PGF datasets series makes them suitable for analyses of trend and variability in precipitation and *PET* across small-sized catchments like the study area. Therefore, this study aimed at analysing the changes in precipitation and PET based on PGF dataset series across the two catchments of Lokok and Lokere in the northeastern Uganda.

2 Study area, data and methods

2.1 The study area

The study area encompasses two catchments (Lokok and Lokere) bordering each other (Fig. 1). The catchments are in the Karamoja and Teso regions, in the northeastern Uganda. Lokok has a catchment area of about 5531 km^2, whereas Lokere is nearly 8178 km^2 totalling to a drainage area of about 13,709 km^2, entirely restricted within the borders of Uganda (see Fig. 1). The two catchments stretch from the Karamoja region covering six districts of Moroto, Kotido, Napak, Abim, Nakapiripirit and Kaabong, to the Teso region covering two districts (Amuria and Katakwi) (Ministry of Water and Environment, 2016). Lokok and Lokere are part of the 11 Kyoga Water Management Zone (KWMZ) catchments (Ministry of Water and Environment, 2017), with drainage areas stretching between latitudes 1° 40′ N and 3° 40′ N and longitudes 33° 30′ E and 34° 60′ E. To the west, Lokok shares border with Aswa catchment which is part of the Upper Nile Water Management zone. To the East and South, Lokere borders Awoja and Akweng catchments, respectively. Awoja and Akweng catchments are also part of the KWMZ. In the study area, short and more intense rainfall occurs from April to July. The second and less intense rainfall occurs between September and December/January (Ministry of Water and Environment, 2017). The average annual rainfall ranges between 500 and 1250 mm.

The area is mainly occupied by Iteso, Kumam, Karamajong and Langо as the major cultural tribes. The study area is among the poorest in Uganda (Ministry of Finance and Economic Planning, 2014), partly due to hostile weather conditions (Ministry of Water and Environment, 2017), which result in high levels of food and nutrition insecurity and low development. The area land comprises cropland, savannah grasslands, woodlands, thickets and shrublands. The diverse landscape favours pastoral and agro-pastoral, the main economic activities of the region's inhabitants. The community also practices sedentary crop production. However, these economic activities suffer from interannual climate variability (Ministry of Water and Environment, 2017), which is the major constraints resulting in recurrent water shortages, hence, crop failure. The variability of weather patterns such as intense rainfall results in disastrous floods, followed by prolonged dry spells and intense drought (Egeru et al., 2014). Generally, the catchment annual evapotranspiration ranges between 300 and 1400 mm and is associated to vegetation, open water bodies, rainfall and temperature (Kigobe and Griensven, 2010; Ministry of Water and Environment, 2017). It is noticeable that the elevation ranges from about 1000 to 3050 m above sea level. The highest point is the peak of Mount Moroto.

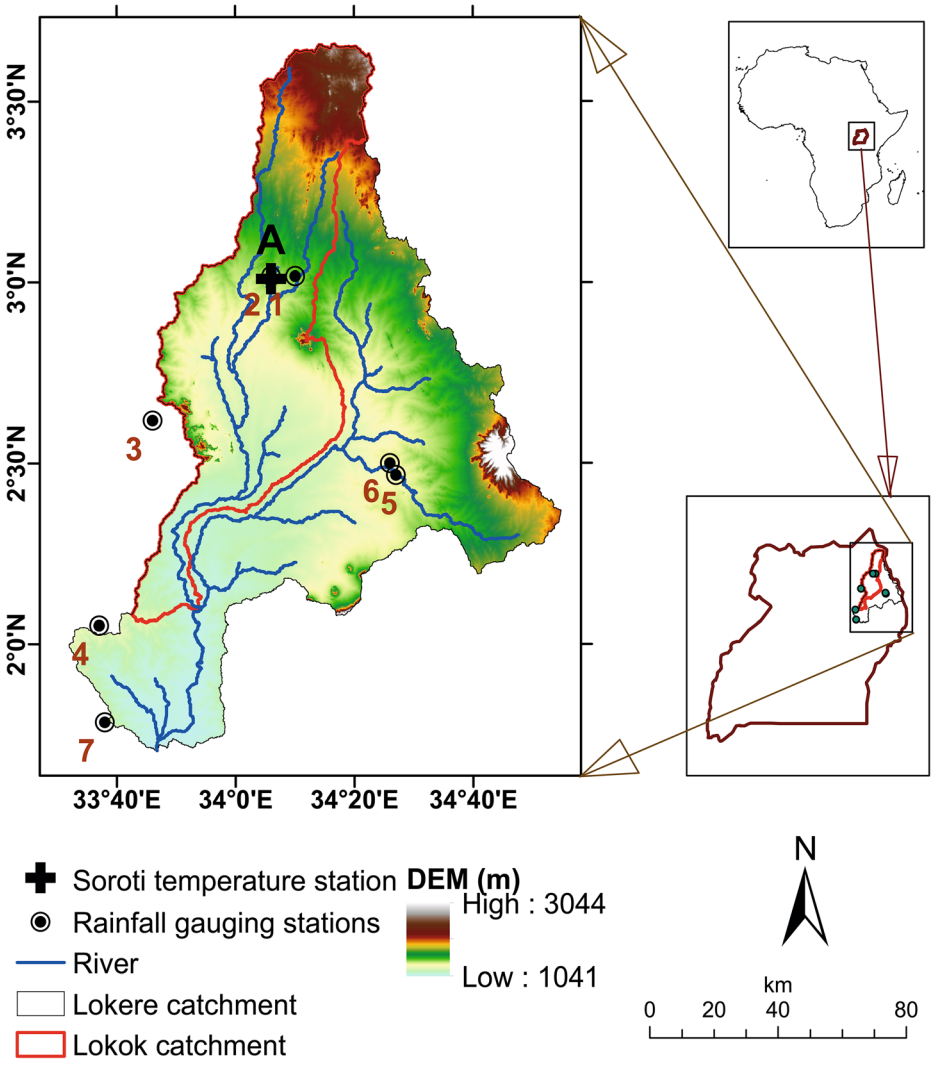

Fig. 1 The Lokok and Lokere catchments. The background map is the digital elevation model (DEM) acquired via http://srtm.csi.cgiar.org/ (accessed: 15 August 2020)

The presence of topographic features like Mount Moroto results into orographic influence on precipitation inducing processes (Ministry of Water and Environment, 2017). In addition, soils are in general fertile, but sensitive to soil erosion. In the low-lying flat areas, the existence of soils with a very low penetration capacity results in waterlogging.

2.2 Data

2.2.1 Precipitation and PET

Daily precipitation and minimum (T_{min}) and maximum (T_{max}) temperature data of the observational-reanalysis hybrid PGF (Sheffield et al., 2006) were obtained in a gridded

(0.25° × 0.25°) form from http://hydrology.princeton.edu/data/pgf/v3/0.25deg/ (accessed: 28 August 2020). The acquired PGF data for the entire 69 years starting from 1948 and ending 2016 possessed no missing values. This data was hitherto used in several studies such as Mubialiwo et al. (2020) and Onyutha et al. (2020). Prior to its use, the PGF-based data was validated (using rainfall data from seven measuring stations (Table 1)) in a similar way as performed in recent studies by Mubialiwo et al. (2020), Onyutha et al. (2020) and Onyutha (2016a) (see sub-sections 2.5 and 3.3 for details). Daily observed rainfall data were obtained from the Uganda National Meteorological Authority (UNMA). From Table 1, it is noticeable that most stations have data records ending in the 1980s, except the Arapai Agric. College station with data up to 1999. Lack of data in the years after 1999 is attributed to the civil war that happened in the 1980s, resulting in destruction of weather stations across Uganda, according to the Japan International Cooperation Agency (JICA) (2011). Therefore, since validation required the same period of PGF and observed data, the period from 1948 to 1999 is considered here.

Missing values for the rainfall data stations were filled-in (using the inverse distance weighted (IDW) interpolation technique (Shepard, 1968)) as applied in the previous study by Mubialiwo et al. (2020).

Similarly, the daily observed temperature data at Kotido station A (Fig. 1) was used to validate the nearby PGF-based T_{min} and T_{max} that were later used to approximate PET. Data observed from Kotido weather station was obtained from the Uganda National Meteorological Authority (UNMA). The observed temperature data covered a period from 1948 to 1982 (35 years). Like the rainfall data, missing values in the Kotido station temperature series were filled-in (using the inverse distance weighted (IDW) interpolation technique (Shepard, 1968). From Fig. 2 a and b, an annual bimodal pattern in observed temperature at Kotido is evident. The corresponding PGF-based temperature data exhibited a unimodal pattern (Fig. 2a, b). The average observed T_{max} and T_{min} were correspondingly 30.4 °C and 19.0 °C, whereas the PGF-based average T_{max} and T_{min} were 26.7 °C and 26.3 °C, respectively. A very small difference between PGF-based average T_{max} and T_{min} (0.4 °C) is noticeable compared to that in the observed temperature data (11.4 °C). The monthly *PET* values computed using the PGF-based T_{max} and T_{min} data was largely underestimated compared to the ones obtained using the observed temperature data (Fig. 2c). The underestimation of *PET* is attributed to the negligible difference between the PGF-based T_{max} and T_{min}. The PGF-based *PET* were lower than the observed *PET* by about 40%. However, the observed and PGF-based PET possess similar pattern (Fig. 2c). This is comparable to the results found by Onyutha et al. (2020) when comparing PGF-based T_{max} and T_{min} against observed temperature at Soroti and Jinja stations.

Table 1 Rainfall station, their coordinates, data record period and missing records

S/N	Station name	Coordinate		Data record		Missing record (%)
		Latitude	Longitude	From	To	
1	Kotido PWD	3.02	34.17	1948	1980	12.2
2	Kotido	3.02	34.10	1948	1985	11.4
3	Morulem	2.62	33.77	1951	1989	8.6
4	Kuju VTC	2.05	33.62	1957	1977	1.2
5	Kangole	2.47	34.45	1948	1990	14.4
6	Kangole Catholic Mission	2.50	34.43	1956	1988	9.8
7	Arapai Agric. College	1.78	33.63	1965	1999	6.7

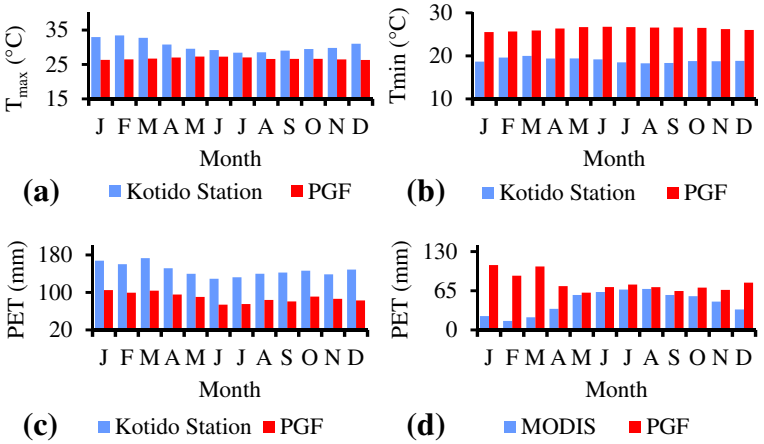

Fig. 2 Comparison of mean monthly (**a**) T_{max}, (**b**) T_{min}, (**c**) PET at Kotido weather station and (**d**) MODIS PET and the PGF-based data. In Fig. 2c the PGF-PET was computed at station point, while in Fig. 2d it is an aerial average over the study area

The underestimation of *PET* signalled the need for refining the quality of PGF data in reproducing temperature data (especially minimum temperature) over the study area.

Only one station for observed temperature (Kotido) was used to validate the PGF-based temperature data due to lack of other temperature observing stations within the study area. Several reanalyses or satellite temperature and precipitation products exist. Examples of such datasets include the Climate Research Unit CRU TS (Harris et al., 2020, 2014) and the Moderate resolution Imaging Spectrometer (MODIS) (Running et al., 2017), which can be used to validate the PGF dataset. In this study, MODIS PET series from 2000 to 2014 adopted from the report by Ministry of Water and Environment (2017) were also used to validate the PGF-based PET. Here, catchment-wide average PGF-based PET were used. A close agreement is noticeable between MODIS and PGF-based PET from May to November. However, there is mismatch between MODIS and PGF-based PET from December to April (Fig. 2d). This mismatch could be attributed to several shortcomings including bias and random errors resulting from numerous factors such as sampling rate, inadequate spreading of sensors and uncertainties in the retrieval algorithms (Ehret et al., 2012). For instance, MODIS data has several limitations including inaccuracy of input algorithm (like Leaf Area Index and EVI) (Miranda et al., 2017). Besides, the CRU TS *PET* data are in the form of countrywide average series (Harris et al., 2020, 2014), hence considered coarse with respect to the catchment size of the current study area.

This study was based on estimated *PET* from PGF-based T_{max} and T_{min} because of the absence of observed long-term evaporation data over the study area. Several methods for estimating *PET* have been developed and categorised as mass transfer-based, e.g. Rohwer (1931); temperature-based, e.g. Hargreaves (Hargreaves and Samani, 1985, 1982), Hamon (1963), Thornthwaite (1948), Blaney–Criddle (1950) and Linacre (1977); radiation-based such as Makkink (1957), Priestly-Taylor (Priestley and Taylor, 1972) and Abtew (1996); and combined energy-mass balanced including the Penman–Monteith (PM) (Allen et al., 1998). Despite its wide application of Penman–Monteith method (Allen et al., 1998; Aouissi et al., 2016) as a standard *PET* estimation method because of its physical and aerodynamic meaning, the method requires highly detailed weather data, making it inappropriate for regions with

scarce data (Lang et al., 2017). Therefore, for regions with scarce weather data challenges, the study area included simple methods such as Hargreaves (Hargreaves and Samani, 1985, 1982) which are recommended for estimation of *PET* (Lingling et al., 2013). Based on the semi-arid climate of the study area (Egeru et al., 2019, 2014), either the Hargreaves (Hargreaves and Samani, 1985, 1982) or Blaney–Criddle (Blaney and Criddle, 1950) methods which are developed for arid or semi-arid climates (Lang et al., 2017) are best suited to estimate the *PET*. Hargreaves and Allen (2003) established that the Hargreaves method requires only minimum and maximum temperature data, is simple to apply, and is less affected in situations when data is obtained from arid or semi-arid, unirrigated sites than the Penman–Monteith method.

Aouissi et al. (2016) evaluated the performance of Penman–Monteith (PM) (Allen et al., 1998), Hargreaves (Hargreaves and Samani, 1985, 1982) and Priestly-Taylor (1972) methods in estimating *PET*. The Hargreaves method generated streamflow estimates close to the observations when applied to the Joumine basin in northern Tunisia (Aouissi et al., 2016). The study by Li et al. (2018) compared the performance of Hargreaves with the standard Penman–Monteith method in simulating streamflow in the Ganjiang River Basin in southern China. The study revealed commendable performance of the Hargreaves method (Li et al., 2018). Lang et al. (2017) compared with three radiation-based methods including the Makkink, Abtew and Priestley–Taylor and five temperature-based methods of Hargreaves, Thornthwaite, Hamon, Linacre and Blaney–Criddle with the Penman–Monteith. Whereas the radiation-based methods performed better than the temperature-based methods, the Hargreaves method performed best among the temperature-based methods when applied to several basins in southern China (Lang et al., 2017). Gao et al. (2017) applied seven PET estimating methods, and Hargreaves included the arid region of Aksu, China, semi-arid region of Tongchuan, China, and humid region of Starkville, MS, USA. The Hargreaves methods performed best in the arid and semi-arid regions (Gao et al., 2017). Najmaddin et al. (2017) applied four methods including Hargreaves, using the Penman-Monteith as the benchmark to estimate PET over Kurdistan Region in northeastern Iraq. The Hargreaves method yielded accurate and unbiased PET estimates for semi-arid regions (Najmaddin et al., 2017). Li et al. (2018) further established that the Hargreaves method is more applicable over arid and semi-arid regions. In Uganda, the Hargreaves method was applied for analysis of variability in evapotranspiration across Lake Kyoga (Onyutha et al., 2020), assessment of decadal or multi-decadal variation in evapotranspiration in Mpologoma catchment (Mubialiwo et al., 2020).

The Hargreaves method was recently applied by Onyutha et al. (2020) in the study to evaluate PET changes over Lake Kyoga Basin where the study area is situated. Another study by Mubialiwo et al. (2020) applied the Hargreaves method to estimate PET over the Mpologoma catchment which is located in the same zone (KWMZ) with the study area. Henceforth, based on its simplicity, the minimum data requirement (T_{max}*and* T_{min} and latitude) by the Hargreaves method, coupled with its recent application in the KWMZ (Mubialiwo et al., 2020; Onyutha et al., 2020), where the study area is located, the Hargreaves method was adopted in this study. PET was estimated using the following equation:

$$PET = 0.0023 \times Ra \times \sqrt{(T_{\max} - T_{\min})} \times (T_{\text{mean}} + 17.8) \quad (1)$$

where PET has units of mm/day and R_a stands for extra-terrestrial solar radiation of the crop surface measured in Wm^{-2}. The latitude at each grid and the calendar day of the year are used to estimate the R_a. T_{mean} is the mean temperature measured in $^{\circ}C$.

The daily precipitation and computed PET were transformed into seasonal and annual totals. Four seasons were considered including March–May (MAM), June–August (JJA), September–November (SON) and December–February (DJF). Correspondingly, at each rainfall station, annual and seasonal (MAM, JJA, SON, DJF) time series were extracted.

2.3 Trend analyses

Trend magnitude or slope (m) in seasonal and annual precipitation and *PET* was computed at each grid using (Sen, 1968; Theil, 1950):

$$m = median\left(\frac{x_j - x_i}{j - i}\right), \text{for all } i < j \tag{2}$$

where n is the sample size while x_j and x_i are respectively the j^{th} and i^{th} value from the sample size of either precipitation or PET rates such that $1 < i \leq (n-1)$ and $1 < j \leq n$.

Subsequent to the computation of trend magnitude, the non-zero slope significance of the linear change in the precipitation and evapotranspiration was evaluated. To test the significance of trend slopes, a number of methods exist such as the Mann–Kendall (MK) (Kendall, 1975; Mann, 1945) and Spearman rank correlation (Lehmann, 1975; Sneyers, 1990; Spearman, 1904) tests. Another method to test significance of trend slope is by using the cumulative sum of the difference (CSD) between exceedance and non-exceedance counts of data points (Onyutha, 2016a, 2016b, 2016c). The CSD method utilises both the statistical and graphical approaches of trend analyses, yet the other methods (like MK) are purely statistical. Furthermore, the CSD method can be applied to analyse both trends and variability (Onyutha, 2018). The method has been applied by Xu et al. (2020), Mubialiwo et al. (2020), Onyutha et al. (2020), Cengiz et al. (2020), Chen et al. (2019), Vido et al. (2019), Pirnia et al. (2018) and Tang and Zhang (2018). Thus, the CSD was adopted for this study.

To apply CSD method to the given time series of sample size n, first a new time series D_i is obtained as the difference between the exceedance and non-exceedance counts of data points as follows (Onyutha, 2016c):

$$D(i) = Y_a(i) - Y_b(\mathrm{i}) \quad \text{for } i = 1, 2, \ldots, n \tag{3}$$

where $Y_a(i)$ is the number of times each data point is exceeded and $Y_b(i)$ the number of times each data point surpasses others. D was computed to nonparametrically rescale the given time series of size n. The $D(i)$ values are accumulated to attain the cumulative sum which enables the separation of sub-trends over unknown periods of rise and decline in each dataset.

The trend statistics T_{CSD} is obtained as follows (Onyutha, 2016c):

$$T_{CSD} = \frac{6}{(n^3 - n)} \sum_{i=j}^{n-1} \sum_{i=1}^{j} D(i) \tag{4}$$

$T_{CSD} > 0$ and $T_{CSD} < 0$ indicate an upward and downward trend, respectively.

Trend statistics T_{CSD} is computed to assess the existence of either monotonic trends or seasonal components in hydrometeorological series, which guides its further use, for instance in hydrodynamic modelling.

The trend statistics T_{CSD}can then be standardised to have a normal distribution with mean of zero and variance of $(n\text{-}1)^{-1}$ as in the following equation (Onyutha, 2016b, 2016d):

$$Z_{CSD} = T_{CSD}\left(\sqrt{(n-1)^{-1} \times \lambda}\right)^{-1} \tag{5}$$

where Z_{CSD} is the standardised trend statistics of T_{CSD} having mean (variance) of zero (one), and λ is the parameter to remove the effect of autocorrection from the variance trend statistics T_{CSD} (Onyutha, 2017). The CSD test was applied to the precipitation and PET data at each grid. Based on the considered level of significance α in this study, the null hypothesis H_o (no trend) was rejected when the computed absolute value of Z_{CSD} was greater than the absolute value of the standard normal variate $Z_{\alpha/2}(|Z_{CSD}| > |Z_{\alpha/2}|)$; otherwise, the H_o was not rejected.

2.4 Variability analyses

Variability in seasonal and annual precipitation and *PET* was calculated by applying Eq. (5) that computed the sub-trend statistics Z_{CSD} as clearly described by Onyutha (2018). In this way, X is assumed to contain a subset x starting from the k^{th} to thew^{th} value of X. To achieve this, subsets were extracted using a window of length q from the start covering-up to the end of the data series. In brief, for the chosen q, $y = 0.5 \times (q + 1)$ and $y = 0.5 \times q$ for the scenarios when q is respectively considered odd and even. q is the considered relevant time scale. For instance, q =10 would represent assessment of decadal oscillations effect:

$$Z^{q}_{CSD(t)} = f\left(x \subset X | x_k \le x \le x_w\right) \quad for\ t = 1, 2, \ldots, n \tag{6}$$

where $Z_{CSD(t)}$ is the t^{th} value of Z_{CSD}, while the parameters k and w can be obtained from:

$$\left.\begin{array}{l} \text{if } t < y, \quad \text{k} = 1, \quad \text{w} = q + t - y - 1 \\ \text{if } t \ge y \text{ and } t \le (n-y), \quad \text{k} = t - y + 1, \quad \text{w} = t + y \\ \text{if } t > (n-y) \text{ and } t \le n, \quad \text{k} = t - y + 1, \quad \text{w} = n \end{array}\right\} \tag{7}$$

To evaluate the natural randomness of the H_o, the values of $Z_{CSD(t)}$ in Eq. (6) are plotted against the matching t^{th} data year and the (100-α) % confidence interval (CI) limits created using the values of $\pm Z_{\alpha/2}$ at α. The line $Z_{CSD} = 0$ is regarded as the reference implying totally no trend in the data series. Variability in the precipitation and evapotranspiration data is signalled by the existence of positive or negative sub-trends in different sub-periods. Depending on the selected significance level α in this study (5%), the H_o was rejected when the scatter plots outside the (100-α) % CI limits or when the $|Z_{CSD}| > Z_{\alpha/2}$; otherwise, the H_o was not rejected. CI is computed to test the significance of trend.

2.5 Correlation analyses between observed precipitation and PGF-based precipitation

The relationship between seasonal and annual observed rainfall from the seven selected stations and their corresponding nearby PGF precipitation was determined and results presented both statistically and graphically. The relationship was assessed by testing the H_o (no correlation between PGF-based precipitation and observed rainfall) at a significance level α of 5%. As observed from Table 1, majority of the stations have data records ending in the 1980s, apart from Arapai Agric. College station whose data goes up to 1999. Therefore, since validation required the same period of PGF and observed data, the period from 1948 to 1999 is considered here.

3 Results and discussion

3.1 Trend and sub-trends in precipitation and PET

Figure 3 shows linear trend magnitude in precipitation and PET at MAM and annual time scales. The linear trend in JJA, SON and DJF seasons is included in Supplementary Material Fig. M1. The entire study area was characterised by a decreasing trend in both MAM (Fig. 3a) and annual (Fig. 3b) precipitation. These results are in treaty with the finding by Onyutha et al. (2020) for MAM season over a period of 1961 to 2008. The largest decrease in precipitation of about −1.45 mm/year and − 1.26 mm/year for MAM (Fig. 3a) and annual (Fig. 3b) time scales, respectively, was found in the northern part of the study area. Similarly, during the JJA, SON and DJF seasons, the entire study area was characterised by a decreasing trend in precipitation (Supplementary Material Fig. M1(a-c)). MAM precipitation had the highest trend slopes compared to the other time series. Both seasonal and annual PET were mainly characterised by an increasing trend, except in the southern part (Fig. 3c, d, and Supplementary Material Fig. M1 (d-f)). The study by Onyutha et al. (2020) reported similar results for MAM, SON and annual *PET* over a period of 1961 to 2008. Kisembe et al. (2019) and Kansiime et al. (2013) also reported rainfall decrease in the northeastern part of Uganda and Lake Kyoga basin, respectively. The study by Ongoma and Chen (2017) established that rainfall over the study area exhibited a significant decrease particularly from the 1980s to 2000s.

Figure 4 shows the standardised trend statistics Z for MAM and annual time series corresponding to the trend slope values in Fig. 3. In the Supplementary Material Fig. M2, results of standardised trend statistics Z for the JJA, SON and DJF season are provided. Over the entire area, H_o (no trend) was rejected ($p < 0.05$) for MAM (Fig. 4a) and annual (Fig. 4b) precipitation. Similarly, JJA, SON and DJF precipitation over the entire study area had H_o (no trend) rejected ($p < 0.05$) (Supplementary Material Fig. M2(a-c)).

The MAM PET had the H_o (no trend) not rejected ($p > 0.05$) over the entire study area with corresponding standardised trend statistics Z values range of $-0.66 \leq Z \leq 1.41$ (Fig. 4c). Similarly, except some parts in the northern region where the standardised trend statistics Z values was slightly above the standard normal variate $Z_{\alpha/2}$ of 1.96 at α of 0.05, the annual PET had the H_o (no trend) not rejected ($p > 0.05$) (Fig. 4d). Generally, JJA PET had the H_o (no trend) not rejected ($p > 0.05$) over the entire study area (Supplementary Material Fig. M2(d)). However, largely, SON PET had the H_o (trend) rejected ($p < 0.05$) except in the central parts of the study area (Supplementary Material Fig. M2(e)). On the other hand, DJF PET had the H_o (trend) rejected ($p < 0.05$) in the northern and H_o (trend) not rejected ($p > 0.05$) in the southern

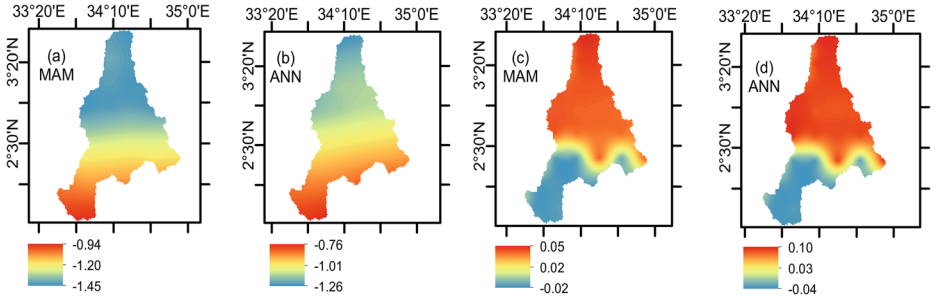

Fig. 3 Trend slope (mm/year) for (**a**, **c**) MAM and (**b**, **d**) annual in (**a**, **b**) precipitation and (**c**, **d**) PET

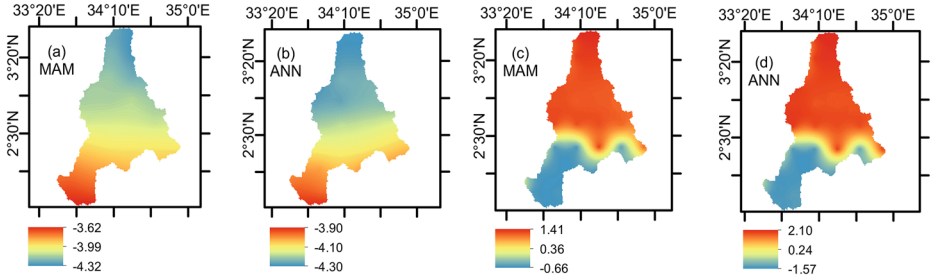

Fig. 4 Standardised trend statistics Z for (**a**, **b**) precipitation and (**c**, **d**) *PET* at (**a**, **c**) MAM and (**b**, **d**) annual time scales

region (Supplementary Material Fig. M2 (f)). It is noticeable that for both seasonal and annual time scales, the spatial results of trend across the entire study area whether in precipitation or PET were clear. The values of standardised trend statistics Z are summarised in Table M1 of the Supplementary Material.

A decrease in precipitation together with an increase in PET (especially in the central to northern region of the study area) could imply occurrence of a prolonged dry spell and hydrological and agricultural drought. Consequently, the already poorest region (Ministry of Finance and Economic Planning, 2014) stands a risk of being more stressed due to high levels of food and nutrition insecurity. Hence, predictive planning of the water resources management applications would necessitate consideration of nonstationary due to the presence of trends and changes in the precipitation, and *PET* (Salas and Obeysekera, 2014). Additionally, with pastoralism, agro-pastoralism and sedentary crop production as the major economic activities in the area, the community may need to develop resilient mechanisms such as storing water during the rainy seasons for use when the prolonged dry spell and drought strides. Drought resistant grass could as well be adopted by the pastoralists.

3.2 Spatio-temporal variability analyses on precipitation and PET

Figures 5 and 6 show the spatio-temporal variations in the annual (Fig. 5) and MAM (Fig. 6) precipitation. The spatio-temporal variations in JJA, SON and DJF seasons can be found in Figs. M3 to M5 of the Supplementary Material. The entire study area was characterised by different but insignificant fluctuations in time (H_0 not rejected) (Fig. 5 (a)), of largely comparable pattern (Fig. 5 (b–g)) considering the annual time scale. Previously, the study by Onyutha (2016a) that was conducted over the entire Uganda at annual scale reported comparable results. Annual precipitation was above the long-term mean in the 1950s as well as from the early 2000 till the end of the study period (2016). However, from early 1960 till the late 1990s, annual precipitation was below the long-term mean. Generally, the pattern from the early 2000 to 2016 had weak amplitude compared to the one in 1950s. Largely, precipitation was below the reference datum (Fig. 5 (b–g)). The study by Egeru et al. (2014) reported predominance of dryness intensity from 1979 to 1995 within the Karamoja region where the study area is largely located. The same study reported occurrence of wetness intensity from 2003. Previous studies (Dias et al., 2015; Mo et al., 2015; Parr et al., 2016) established a relationship between changes PET with various factors, land cover changes included. Similarly, it has been documented (Dorji et al., 2016; Mmbando and Kleyer, 2018; Napoli et al., 2019) that trend and variability in precipitation may vary from one altitude to another. Furthermore, Parr et al. (2016) stressed out that changes in precipitation may result in variations in PET.

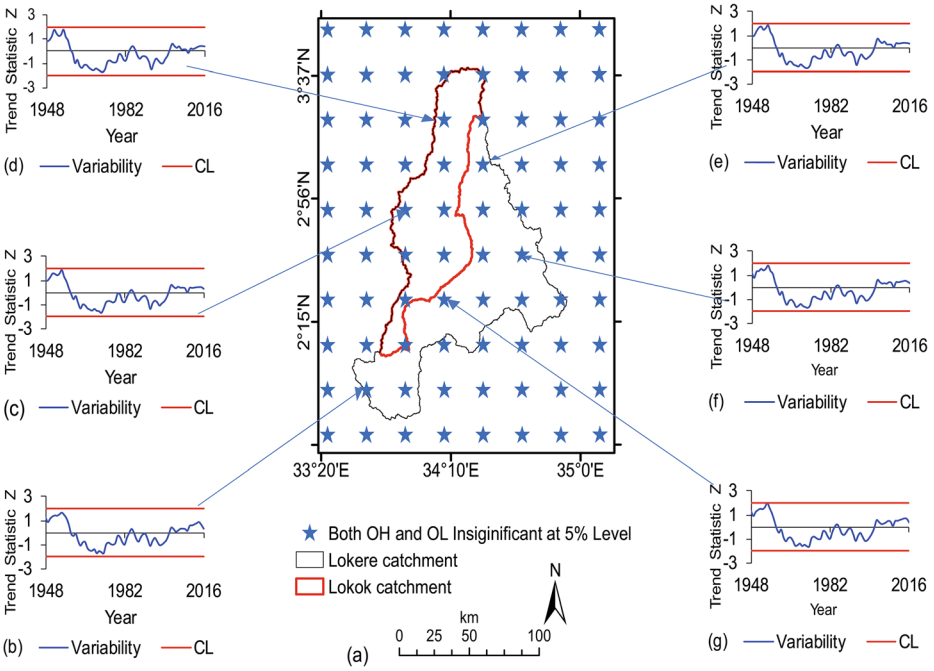

Fig. 5 (a) The spatial changes in the significance of precipitation variability and (b–g) the temporal variability in annual precipitation from different parts of the study area. "CL" corresponds to the dotted horizontal lines denoting the 95% confidence interval limits

The MAM precipitation over the entire study area exhibited significant OH (H_0 rejected) of generally strong amplitude at 5% level. The far southeast and some parts in the West (outside the study area) experienced both insignificant OH and OL (H_0 not rejected). Like the annual temporal variation, MAM precipitation was above the long-term mean in the 1950s as well as from the early 2000 till 2016. Still, from early 1960 till the late 1990s, MAM precipitation was below the long-term mean. It is most likely that the prolonged dry spells and extreme hydrological and agricultural drought in the study area could be linked to reduced precipitation as indicated by more OL than OH. This is in line with the findings from Ongoma et al. (2016) that established low values of simple daily intensity index, an indication of prolonged dry spell and/or drought.

Significant OL (H_0 rejected) were exhibited in the northern parts (mainly outside the study area), while the rest of the area experienced both insignificant OH and OL in JJA precipitation (Supplementary Material Fig. M3(a)). JJA precipitation was characterised mostly by a decline from the early 1960s till end of the study period (2016) at different stations in the study area. However, in the 1950s, precipitation was above the long-term mean (Supplementary Material Fig. M3(b-g)). SON precipitation over the entire study area exhibited both insignificant OH and OL of largely weak amplitude (Supplementary Material Fig. M4(a)). The temporal variation of SON precipitation displayed more pronounced decrease (Supplementary Material Fig. M4(b-g)). DJF precipitation had a similar spatio-temporal variation to that exhibited by the SON season (Supplementary Material Fig. M5(a-g)). It is noticeable from the time plots of selected grid points that precipitation over the study area had very similar temporal variation in the period 1948–2016.

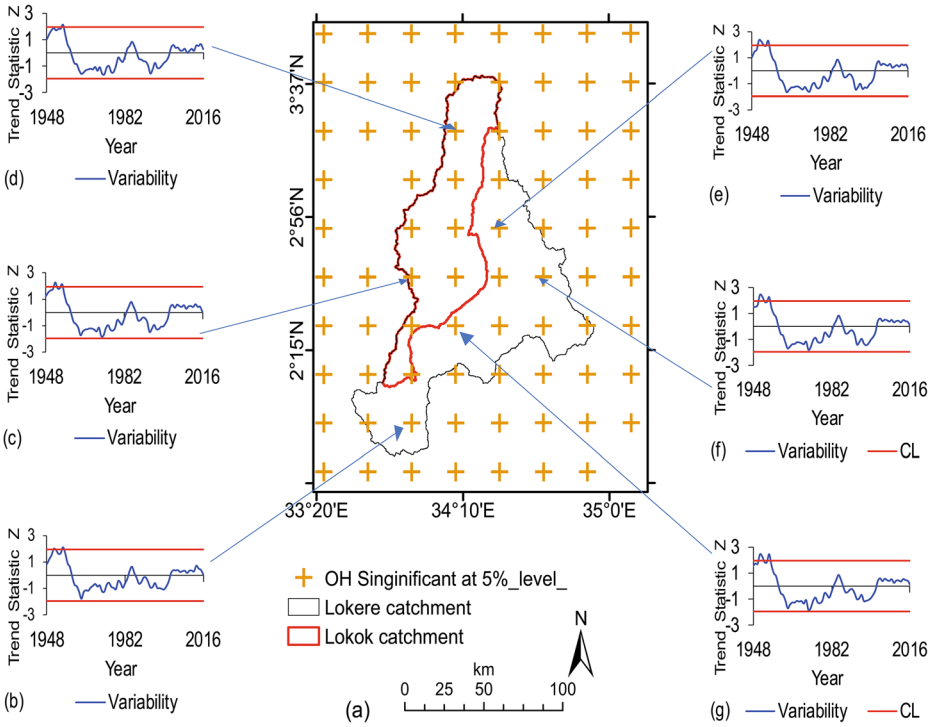

Fig. 6 (a) The spatial changes in the significance of precipitation variability and (b–g) the temporal variability in MAM precipitation from different parts of the study area. "CL" corresponds to the dotted horizontal lines denoting the 95% confidence interval limits

The differences in spatio-temporal variations in annual PET across the area are shown in Fig. 7, respectively. Figs. M6 to M9 of the Supplementary Material show the spatio-temporal variations in MAM, JJA, SON and DJF seasons. Considering the annual PET, Fig. 7 (a) shows that the entire study area experienced both insignificant OH and OL (H_0 not rejected) at the 5% level. The western and southern regions were characterised by similar temporal pattern of weak amplitude (Fig. 7 (b–c)). Annual PET was largely oscillating along the reference, except from the early 2000 till the end of the study period when it was more above the long-term mean (Fig. 7 (b–c)). Equally, the northern, central and western regions had annual PET oscillating along the long-term mean from 1948 till the early 1980s as well as from around 2006 to 2016. However, from around 1985 to till the early 2000s, the annual PET was above the long-term mean (Fig. 7 (d–g)).

The MAM PET was characterised by both insignificant OH and OL (H_0 not rejected) at $\alpha = 0.05$ over the entire area (Supplementary Material Fig. M6(a)), fluctuating above and below the reference for the entire study period ((Supplementary Material Fig. M6(b-g)). The southern and western regions exhibited more of an increase from the early 2000 till the end of the study period (2016) ((Supplementary Material Fig. M6(b-g))). The northern and central parts of the study area had significant OH (H_0 rejected). The rest of the area experienced both insignificant OH and OL in JJA PET (Supplementary Material Fig. M7(a)). JJA PET was characterised by both increase and decrease for the entire study period, but more of the increase occurred in the 1950s (Supplementary Material Fig. M7(b-g)). During the SON

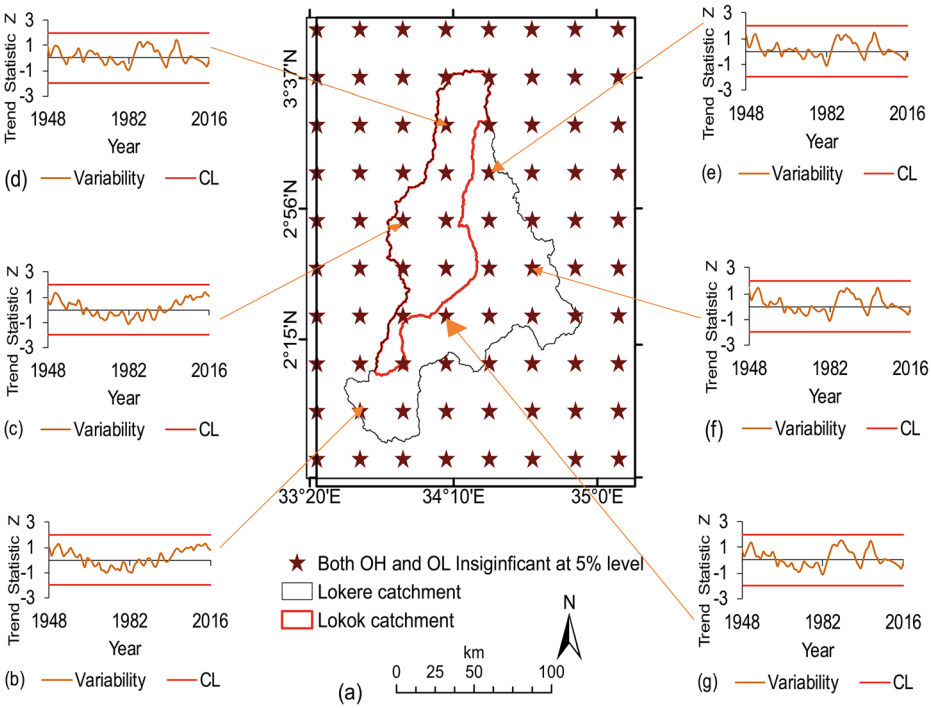

Fig. 7 (a) The spatial changes in the significance of PET variability and (b–g) the temporal variability in annual PET from different parts of the study area. "CL" corresponds to the dotted horizontal lines denoting the 95% confidence interval limits

season, only the area in the northeastern part of the study area experienced significant OH in PET. The rest of the study area had both insignificant OH and OL during the SON season (Supplementary Material Fig. M8(a)). The temporal variation of SON PET was characterised by both increase and decrease (Supplementary Material Fig. M8(b-g)) at different stations in the study area. The southern and western regions experienced more of an increase from the early 2000s till end of study period (2016), while the northern, central and eastern regions portrayed more decrease in PET during the same period. The entire study area experienced both insignificant OH and OL during the DJF season (Supplementary Material Fig. M9(a)). Largely, PET oscillated along the reference (except from about 1984 till end of study period) when a strong variability was exhibited especially in the northern, central and eastern regions (Supplementary Material Fig. M9(d-g)).

3.3 Correlation analysis between observed rainfall and PGF-based precipitation

Following the criteria in sub-section 2.5, the H_o (no correlation between observed rainfall and PGF-based precipitation) was rejected if the absolute correlation coefficient between observed rainfall and PGF-based precipitation is greater than the critical value of correlation at a significance level α of 5%. In this study, correlation between station values and PGF grid point values were computed considering the grid point closest to each station. Herein, correlation is presented statistically (Table 2) and graphically (Fig. 8 and Supplementary Material Figs. M10 to M13). Detailed information about the stations can be found in Table 1.

Table 2 Correlation between annual and seasonal PGF-based precipitation and observed rainfall

Station	Correlation coefficient					Corr. Crit
	Annual	MAM	JJA	SON	DJF	
1	−0.29	−0.38*	−0.59*	−0.61*	0.37*	0.34
2	−0.23	−0.15	−0.59*	−0.54*	0.39*	0.32
3	−0.49*	−0.54*	−0.32	0.03	0.68*	0.32
4	0.41	0.17	−0.52*	0.25	0.48*	0.43
5	−0.57*	−0.23	−0.67*	0.37*	0.46*	0.30
6	0.33	0.25	−0.38*	0.52*	0.02	0.34
7	0.02	0.17	−0.70*	0.11	0.31	0.33

Corr. Crit stands for critical absolute value of correlation at the 5% significance level

*Denotes significant correlation with the H_0 (no correlation) rejected at α of 5%

The adopted two-tailed test yielded critical values of the correction ranging between 0.30 and 0.43 included (Table 2). From Table 2, it is noticeable that each station had H_0 which was rejected on at least one-time scale. For annual precipitation, H_0 was rejected at two stations 3 and 5, but H_0 was not rejected at stations 1, 2, 4, 6 and 7. For the MAM precipitation, H_0 was rejected at stations 1 and 3, but H_0 was not rejected at stations 2 and 4–7. For both annual and MAM precipitation, stations 1, 2, 3 and 5 exhibited negative correlation, while stations 4, 6 and 7 exhibited positive correlation though insignificant. All stations (except 3 that displayed insignificant negative correlation) had significant negative correlation during the JJA seasons. Stations 1 and 2 had significant negative correlation, while stations 5 and 6 exhibited significant positive correlation during the SON season. Still in the SON season, the other stations 3, 4 and 7 had insignificant positive correlation. Unlike the other time scales, in the DJF season, all stations had positive correlation, with stations 1–5 exhibiting significant correlation. From the results, it can be deduced that PGF data can generally reproduce the DJF and SON precipitation over the study area than the other time scales. In addition, PGF can relatively reproduce precipitation at stations 4, 6 and 7 during MAM and annual time scales. The negative correlation exhibited in the JJA season underscores PGF in reproducing precipitation during the season. The negative correlation whether significant or insignificant

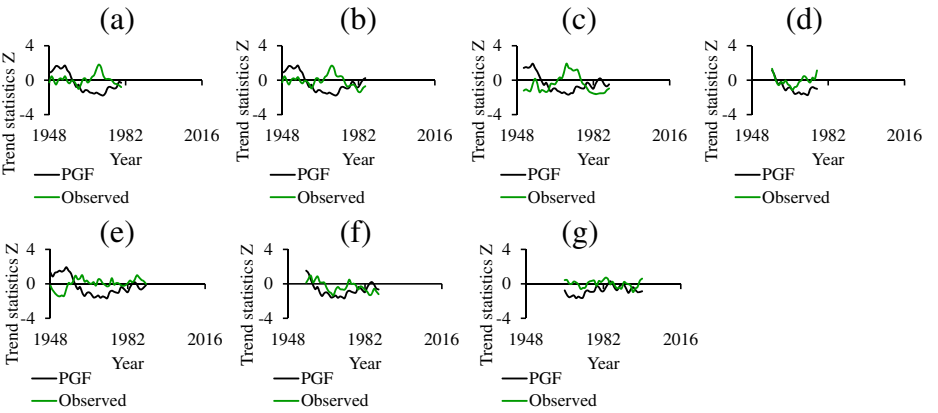

Fig. 8 Comparison of trend statistics Z in annual observed rainfall and PGF-based precipitation on each station

designates that when there is an increase (decrease) in the observed rainfall, the PGF-based precipitation displays a decrease (increase).

The results in Fig. 8 reveal overestimation and underestimation of the fluctuating highs and lows from the annual observed rainfall by the PGF-based rainfall of generally negative correlation. The comparison of trend statistics Z in PGF-based precipitation and observed rainfall at each station during MAM, JJA, SON and DJF seasons can be found in Supplementary Material Figs. M10 to M13. Similar to the observation made in Table 2, graphically, results showed close agreement between PGF-based and observed trend statistics Z during the DJF season (Supplementary Material Fig. M13). Similarly, for the JJA season, a disagreement is observable (Supplementary Material Fig. M11). It is noticeable that the imitation of variability in the observed rainfall by the PGF-based precipitation fluctuates from one station to another. This could be associated to the influence of local features such as mountains and lake such as Lake Kyoga (Camberlin, 2009), which might not be well captured by the PGF. Figure 8 and Supplementary Material Figs. M10 to M13 reveal a noticeable cyclic behaviour of the underestimation and overestimation. This behaviour could be a result of the climate variability influence on precipitation in the catchment, a clear signal of possible severe wetter and drier events (Onyutha, 2016d). Subsequently these OH and OLs neutralise each other (Onyutha, 2016d). A hydrometeorological time series with strong cyclic behaviour may necessitate complex methods such as spectral analysis (Grzesica and Więcek, 2016; Mahmood et al., 2019). Despite the low correlation exhibited at some stations, the use of PGF-based products after some sieving of the disparities in the data using appropriate temporal scale can give a perception on the possible long-term trend and variability, a vital element for predictive planning of adaptation (Onyutha, 2016a).

4 Conclusion

Studies on the analyses of changes in precipitation and *PET* at the catchment level of Lokok and Lokere were lacking by the time of writing this paper. This paper analysed the changes in the long-term (1948–2016) annual and seasonal precipitation and PET over Lokok and Lokere catchments in a gridded (0.25° × 0.25°) form of the PGF data. The analyses of trend and variability were based on the nonparametric CSD technique. The entire study area was characterised by a decreasing trend ($p < 0.05$) in the seasonal (MAM, JJA, SON, DJF) and annual precipitation. Generally, precipitation exhibited positive anomalies in the 1950s as well as from the early 2000 till the end of the study period (2016), except for the JJA season. However, between 1960 and the late 1990s, precipitation was largely below the long-term mean. Generally, the pattern from the early 2000 to 2016 showed a weak decrease compared to the one in 1950s. Largely, precipitation was below the reference datum. Both MAM and JJA PET were characterised by a positive trend ($p > 0.05$), except in the southern part, with negative trend ($p > 0.05$). DJF and annual PET had a positive trend ($p < 0.05$) in the northern region. However, the southern area had a negative trend ($p > 0.05$). The trend in SON PET was respectively positive and negative ($p < 0.05$) in the North and South, while the central region had a positive trend (($p > 0.05$). Both seasonal and annual PET had alternating positive and negative anomalies for the entire study period. An increase in PET (especially in the central to northern region of the study area) in MAM and JJA seasons although largely insignificant, together with a decrease in precipitation, could imply occurrence of prolonged dry spells and hydrological and agricultural drought which result in crop failure hence food insecurity. Consequently, the community is extremely distressed because they depend on pastoral and agro-pastoralism. If such conditions linger into the future, the community in Lokok and Lokere may need to develop resilient

mechanisms such as storing water during the rainy seasons for use in dry periods. Furthermore, drought-resistant grass could as well be adopted by the pastoralists.

The PGF-based precipitation was compared with the observed rainfall from seven stations in terms of correlation, trend and variability. Positive correlation was observed at some stations, while others exhibited negative correlation. Generally, PGF reproduced the DJF and SON precipitation over the study area better than the other seasonal intervals. Negative correlation was exhibited in the JJA which underscores PGF in reproducing precipitation during the season. The negative correlation whether significant or insignificant designates that when there was an increase (decrease) in the observed rainfall, the PGF-based precipitation displayed a decrease (increase). The PGF data overestimated and underestimated the fluctuating highs and lows from the observed rainfall, varying from one location to another. This variability could be linked to the presence of regional features such as water bodies (e.g., Lake Kyoga) and mountains (e.g., Mount Moroto) (Camberlin, 2009). For instance, the study by Thiery et al. (2015) revealed that the East African regional climate is highly influenced by Lake Victoria resulting from induction of circular airflow with over-lake convective inhibition during daytime and an inverted pattern at night. A cyclic behaviour of the underestimation and overestimation was noticeable in precipitation, and it could be attributed to climate variability influence on precipitation. The PGF may be having limitation in accurately capturing the magnitudes of events over epochs characterised by wet and/or dry conditions, and this is based on the scale chosen for analyses Similarly, the monthly mean values of T_{min} and T_{max} of the PGF-based and those observed at the Kotido weather station were compared. The PGF-based data yielded a unimodal pattern, while a bimodal pattern was exhibited by the observed data. The PGF-based data undervalued the difference between the T_{max} and T_{min}, resulting in underestimation of the PGF-based PET values. Furthermore, comparison of PGF-based and MODIS PET was made. A close agreement was noticeable between MODIS and PGF-based PET from May to November. However, there is mismatch between the two datasets from December to April.

Despite the low correlation, application of PGF-based time series for trend and variability analyses after some sieving of the disparities in the data using appropriate temporal scale can still give a perception about the changes in the climate variables (Onyutha, 2016a). Nonetheless, there is need to make enrichment on the quality of PGF data in reproducing the observed climatic data especially over the sub-Saharan Africa which has challenges of low density of meteorological stations.

A few limitations to this study are worth mentioning. The study adopted the uncalibrated empirical Hargreaves method to approximate *PET*. It is likely that the use of uncalibrated empirical Hargreaves method could generate biased results, hence affecting the analyses of trend and variability. To eliminate the impact resulting from using a certain method, it is suggested that future research studies consider the use of more than one method, to estimate PET. Only the CSD method was used in analysing trend and variability of both precipitation and PET over the study area. For trend analyses, other methods such as Mann–Kendall (Kendall, 1975; Mann, 1945) and Spearman's Rho (Lehmann, 1975; Sneyers, 1990; Spearman, 1904) tests exist. For at-site analyses of variability, other methods like the quantile perturbation method (Ntegeka and Willems, 2008) and autocorrelation spectral analysis (ASA) (Blackman and Tukey, 1959) can be employed. To balance out the effect due the choice of a certain method, it is recommended that future research studies on the trend and variability in precipitation and PET over the study area consider more than one approach. While an in-depth exploration of the changes in precipitation and PET for refined results at localised catchment scales (like Lokok and Lokere) is deemed very crucial, this may face challenges of chaotic behaviour of the weather/climate system at local scales, hence deterring derivation of general

conclusions. The findings of this study are vital for planning of predictive adaptation to the effects of climate variability on the water resources management applications. With proper predictive planning, the pastoral and agro-pastoralist community in Lokok and Lokere can reduce on the impact of prolonged dry spell and hydrological and agricultural drought.

Supplementary material The online version of this article (https://doi.org/10.1007/s42865-021-00031-y) contains supplementary material, which is available to authorized users.

Acknowledgements The authors acknowledge the use of Princeton Global Forcings (PGF) gridded data (Sheffield et al., 2006). The observed rainfall used in validating the PGF dataset was obtained from the Uganda National Meteorological Authority (UNMA). The CSD technique used for trend and variability analyses was acquired from https://sites.google.com/site/conyutha/tools-to-download/ (accessed: 30 August 2020). The authors also acknowledge the use of the MODIS PET dataset provided by Ministry of Water and Environment (2017).

Funding The research was financed through the Ph.D. scholarship (Grant No. ACEWM/GSR/4334/11) and MSc. scholarship (Grant No. ACEWM/GSR/5414/11), respectively awarded to the first and second authors by the Africa Center of Excellence for Water Management, Addis Ababa University, Ethiopia.

Data Availability Readers can access data used in this research by contacting the corresponding author.

Declarations

Conflict of interest The authors declare no competing interests.

References

Abtew W (1996) Evapotranspiration measurements and modeling for three wetland systems in south Florida. J Am Water Resour Assoc 32:465–473. https://doi.org/10.1111/j.1752-1688.1996.tb04044.x

Adler RF, Sapiano MRP, Huffman GJ, Wang J-J, Gu G, Bolvin D, Chiu L, Schneider U, Becker A, Nelkin E, Xie P, Ferraro R, Shin D-B (2018) The Global Precipitation Climatology Project (GPCP) monthly analysis (New Version 2.3) and a Review of 2017 Global Precipitation. Atmosphere, vol 9, pp 1–27. https://doi.org/10.3390/atmos9040138

Adnan S, Ullah K, Ahmed R (2020) Variability in meteorological parameters and their impact on evapotranspiration in a humid zone of Pakistan. Meteorol Appl 27:1–10. https://doi.org/10.1002/met.1859

Alemu H, Kaptué AT, Senay GB, Wimberly MC, Henebry GM (2015) Evapotranspiration in the Nile Basin: identifying dynamics and drivers, 2002–2011. Water 7:4914–4931. https://doi.org/10.3390/w7094914

Allen, R.G., Pereira, L.S., Raes, D., Smith, M., 1998. Crop evapotranspiration - guidelines for computing crop water requirements - FAO Irrigation and drainage paper 56. FAO – Food and Agriculture Organization of the United Nations, Rome, Italy

Aouissi J, Benabdallah S, Chabaâne ZL, Cudennec C (2016) Evaluation of potential evapotranspiration assessment methods for hydrological modelling with SWAT — application in data-scarce rural. Agric Water Manag 174:39–51. https://doi.org/10.1016/j.agwat.2016.03.004

Ashouri H, Hsu KL, Sorooshian S, Braithwaite DK, Knapp KR, Cecil LD, Nelson BR, Prat OP (2015) PERSIANN-CDR: daily precipitation climate data record from multisatellite observations for hydrological and climate studies. Bull Am Meteorol Soc 96:69–83. https://doi.org/10.1175/BAMS-D-13-00068.1

Blackman RB, Tukey JW (1959) The measurement of power spectra. Dover Publications, New York

Blaney HF, Criddle WD (1950) Determining water requirements in irrigated areas from climatological and irrigation data, 48th edn. U.S. Soil Conservation Service, Washington, DC

Byakatonda J, Parida BP, Kenabatho PK, Moalafhi DB (2018) Analysis of rainfall and temperature time series to detect long-term climatic trends and variability over semi-arid Botswana. Journal of Earth System Science 127:1–20. https://doi.org/10.1007/s12040-018-0926-3

Camberlin, P., 2009. Nile Basin Climates, in: Dumont, H.J. (Ed.), The Nile: origin, environments, limnology and human use. Springer, Berlin, Germany, pp. 307–333

Cengiz TM, Tabari H, Onyutha C, Kisi O (2020) Combined use of graphical and statistical approaches for analyzing historical precipitation changes in the black sea region of Turkey. Water 12:1–19. https://doi.org/10.3390/w12030705

Chen Q, Chen H, Wang J, Zhao Y, Chen J, Xu C (2019) Impacts of climate change and land-use change on hydrological extremes in the Jinsha River Basin. Water 11:1–25. https://doi.org/10.3390/w11071398

Dias PCL, Macedo MN, Costa HM, Coe MT, Neill C (2015) Effects of land cover change on evapotranspiration and streamflow of small catchments in the Upper Xingu River Basin, Central Brazil. Journal of Hydrology: Regional Studies 4:108–122. https://doi.org/10.1016/j.ejrh.2015.05.010

Dorji U, Olesen JE, Bøcher PK, Seidenkrantz MS (2016) Spatial variation of temperature and precipitation in Bhutan and links to vegetation and land cover. Mt Res Dev 36:66–79. https://doi.org/10.1659/MRD-JOURNAL-D-15-00020.1

Egeru A, Barasa B, Nampijja J, Siya A, Makooma MT, Gilbert M, Majaliwa J (2019) Past, present and future climate trends under varied representative concentration pathways for a sub-humid region in Uganda. Climate 7:1–21. https://doi.org/10.3390/cli7030035

Egeru A, Osaliya R, Macopiyo L, Mburu J, Wasonga O, Barasa B, Said M, Aleper D, Mwanjalolo GM (2014) Assessing the spatio-temporal climate variability in semi-arid Karamoja sub- region in north-eastern Uganda. Int J Environ Stud 71:490–509. https://doi.org/10.1080/00207233.2014.919729

Ehret U, Zehe E, Wulfmeyer V, Warrach-Sagi K, Liebert J (2012) HESS opinions "should we apply bias correction to global and regional climate model data?". Hydrol Earth Syst Sci 16:3391–3404. https://doi.org/10.5194/hess-16-3391-2012

Funk C, Peterson P, Landsfeld M, Pedreros D, Verdin J, Shukla S, Husak G, Rowland J, Harrison L, Hoell A, Michaelsen J (2015) The climate hazards infrared precipitation with stations - a new environmental record for monitoring extremes. Scientific Data 2:1–21. https://doi.org/10.1038/sdata.2015.66

Gao F, Feng G, Ouyang Y, Wang H, Fisher D, Adeli A, Jenkins J (2017) Evaluation of reference evapotranspiration methods in arid, semiarid and humid regions. J Am Water Resour Assoc 53:1–18. https://doi.org/10.1111/1752-1688.12530

Grzesica D, Więcek P (2016) Advanced forecasting methods based on spectral analysis. Procedia Engineering 161:253–258. https://doi.org/10.1016/j.proeng.2016.08.546

Haile GG, Tang Q, Sun S, Huang Z, Zhang X, Liu X (2019) Droughts in East Africa: causes, impacts and resilience. Earth Sci Rev 193:146–161. https://doi.org/10.1016/j.earscirev.2019.04.015

Hamon WR (1963) Computation of direct runoff amounts from storm rainfall. International Association of Sciences Hydrological Publications 63:52–62

Hargreaves GH, Allen RG (2003) History and evaluation of hargreaves evapotranspiration equation. J Irrig Drain Eng 129:53–63. https://doi.org/10.1061/(ASCE)0733-9437(2003)129:1(53)

Hargreaves GH, Samani ZA (1985) Reference crop evapotranspiration from temperature. Transactions - American Society of Agricultural Engineers 1:96–99

Hargreaves GH, Samani ZA (1982) Estimation of potential evapotranspiration. Journal of Irrigation and Drainage Division 108:225–230

Harris I, Jones PD, Osborn TJ, Lister DH (2014) Updated high-resolution grids of monthly climatic observations - the CRU TS3.10 dataset. Int J Climatol 34:623–642. https://doi.org/10.1002/joc.3711

Harris I, Osborn TJ, Jones P, Lister D (2020) Version 4 of the CRU TS monthly high-resolution gridded multivariate climate dataset. Scientific data 7:1–18. https://doi.org/10.1038/s41597-020-0453-3

Huffman GJ, Adler RF, Bolvin DT, Gu G, Nelkin EJ, Bowman KP, Hong Y, Stocker EF, Wolff DB (2007) The TRMM multisatellite precipitation analysis (TMPA): quasi-global, multiyear, combined-sensor precipitation estimates at fine scales. J Hydrometeorol 8:38–55. https://doi.org/10.1175/JHM560.1

JICA, 2011. The development study on water resources development and management for Lake Kyoga Basin in the Republic of Uganda. Kampala

Jury MR (2018) Uganda rainfall variability and prediction. Theor Appl Climatol 132:905–919. https://doi.org/10.1007/s00704-017-2135-4

Kalnay E, Kanamitsu M, Kistler R, Collins W, Deaven D, Gandin L, Iredell M, Saha S, White G, Woollen J, Zhu Y, Chelliah M, Ebisuzaki W, Higgins W, Janowiak J, Mo KC, Ropelewski C, Wang J, Leetmaa A, Reynolds R, Jenne R, Joseph D (1996) The NCEP NCAR 40-year reanalysis project. Bull Am Meteorol Soc 77:437–472. https://doi.org/10.1175/1520-0477(1996)077<0437:TNYRP>2.0.CO;2

Kansiime MK, Wambugu SK, Shisanya CA (2013) Perceived and actual rainfall trends and variability in eastern Uganda: implications for community preparedness and response. Journal of Natural Sciences Research 3:179–195

Kendall MG (1975) Rank correlation methods, 4th edn. Charles Griffin, London

Kigobe M, Van Griensven A (2010) Assessing hydrological response to change in climate: statistical downscaling and hydrological modelling within the upper Nile. In: Swayne DA, Yang W, Voinov AA, Rizzoli A, Filatova T (eds) 2010 International Congress on Environmental Modelling and Software Modelling for Environment's Sake, Ottawa, Canada. InternationalEnvironmentalModelling andSoftware Society(iEMSs), Ottawa, Canada, pp 1–10

Kisembe J, Favre A, Dosio A, Lennard C, Sabiiti G, Nimusiima A (2019) Evaluation of rainfall simulations over Uganda in CORDEX regional climate models. Theor Appl Climatol 137:1117–1134. https://doi.org/10.1007/s00704-018-2643-x

Lang D, Zheng J, Shi J, Liao F, Ma X, Wang W, Chen X, Zhang M (2017) A comparative study of potential evapotranspiration estimation by eight methods with FAO. Water 9:1–18. https://doi.org/10.3390/w9100734

Lehmann EL (1975) Nonparametrics: statistical methods based on ranks. Holden-Day, San-Francisco, Calif, USA

Li B, Rodell M, Sheffield J, Wood E, Sutanudjaja E (2019) Long-term, non-anthropogenic groundwater storage changes simulated by three global-scale hydrological models. Sci Rep 9:1–13. https://doi.org/10.1038/s41598-019-47219-z

Li Z, Yang Y, Kan G, Hong Y (2018) Study on the applicability of the Hargreaves potential evapotranspiration estimation method in CREST distributed hydrological model (version 3.0) applications. Water 10:1–15. https://doi.org/10.3390/w10121882

Linacre ET (1977) A simple formula for estimating evaporation rates in various climates, using temperature data alone. Agric Meteorol 18:409–424. https://doi.org/10.1016/0002-1571(77)90007-3

Lingling Z, Jun XIA, Chong-yu XU, Zhonggen W, Leszek S, Cangrui L (2013) Evapotranspiration estimation methods in hydrological models. J Geogr Sci 23:359–369. https://doi.org/10.1007/s11442-013-1015-9

Mahmood R, Jia S, Zhu W (2019) Analysis of climate variability, trends, and prediction in the most active parts of the Lake Chad basin, Africa. Sci Rep 9:1–18. https://doi.org/10.1038/s41598-019-42811-9

Maidment RI, Grimes D, Allan RP, Tarnavsky E, Stringer M, Hewison T, Roebeling R, Black E (2014) The 30 year TAMSAT African rainfall climatology and time series (TARCAT) data set. Journal of Geophysical Research: Atmospheres 119:10619–10644. https://doi.org/10.1002/2014JD021927

Makkink GF (1957) Testing the Penman formula by means of lysimeters. Journal Institute of Water Engineers 11:277–288

Mann HB (1945) Nonparametric test against trend. Econometrica 13:245–259

Merzdorf, J., 2019. Two decades of rain, snowfall from NASA's precipitation missions [WWW document]. NASA's Goddard Space Flight Center, Greenbelt, Md. URL https://www.nasa.gov/feature/goddard/2019/precipitation-missions-release-two-decades-of-rain-snow-data (accessed 12.7.20)

Meyer-Christoffer, A., Becker, A., Finger, P., Schneider, U., Ziese, M., 2018. GPCC Climatology Version 2018 at 0.25°: Monthly Land-Surface Precipitation Climatology for Every Month and the Total Year from Rain-Gauges built on GTS-based and Historical Data. Global Precipitation Climatology Centre (GPCC).

Ministry of Finance and Economic Planning (2014) Poverty status report 2014: structural change and poverty reduction in Uganda. Ministry of Finance and Economic Planning, Kampala, Uganda

Ministry of Water and Environment (2017) Catchment management plan: Lokok catchment. Ministry of Water and Environment, Kampala, Uganda

Ministry of Water and Environment (2016) Integrated water resources management in Karamoja Addendum to: enhancing Resilience in Karamoja Program (ERKP). Ministry of Water and Environment, Kampala, Uganda

Miranda, R. de Q, Galvíncio JD, Moura M.S.B. de, Jones CA, Srinivasan R (2017) Reliability of MODIS evapotranspiration products for heterogeneous dry forest: a study case of Caatinga. Adv Meteorol 2017:15–14. https://doi.org/10.1155/2017/9314801

Mmbando GA, Kleyer M (2018) Mapping precipitation, temperature, and evapotranspiration in the Mkomazi River Basin. Tanzania Climate 6. https://doi.org/10.3390/cli6030063

Mo X, Liu S, Lin Z, Wang S, Hu S (2015) Trends in land surface evapotranspiration across China with remotely sensed NDVI and climatological data for 1981–2010. Hydrol Sci J 60:2163–2177. https://doi.org/10.1080/02626667.2014.950579

Mubialiwo A, Onyutha C, Abebe A (2020) Historical rainfall and evapotranspiration changes over Mpologoma catchment in Uganda. Adv Meteorol 2020:1–19. https://doi.org/10.1155/2020/8870935

Mwaura FM, Okoboi G (2014) Climate variability and crop production in Uganda. Journal of Sustainable Development 7:159–172. https://doi.org/10.5539/jsd.v7n2p159

Najmaddin PM, Whelan MJ, Balzter H (2017) Estimating daily reference evapotranspiration in a semi-arid region using remote sensing data. Remote Sens 9:1–20. https://doi.org/10.3390/rs9080779

Napoli A, Crespi A, Ragone F, Maugeri M, Pasquero C (2019) Variability of orographic enhancement of precipitation in the Alpine region. Sci Rep 9:1–8. https://doi.org/10.1038/s41598-019-49974-5

Novella NS, Thiaw WM (2013) African rainfall climatology version 2 for famine early warning systems. J Appl Meteorol Climatol 52:588–606. https://doi.org/10.1175/JAMC-D-11-0238.1

Nsubuga FW, Olwoch JM, Rautenbach H (2014b) Variability properties of daily and monthly observed near-surface temperatures in Uganda: 1960–2008. Int J Climatol 34:303–314. https://doi.org/10.1002/joc.3686

Nsubuga FWN, Botai OJ, Olwoch JM, Rautenbach, C.J. de W, Bevis Y, Adetunji AO (2014a) The nature of rainfall in the main drainage sub- basins of Uganda. Hydrol Sci J 59:278–299. https://doi.org/10.1080/02626667.2013.804188

Ntegeka, V., Willems, P., 2008. Trends and multidecadal oscillations in rainfall extremes, based on a more than 100-year time series of 10 min rainfall intensities at Uccle, Belgium. Water Resour Res 44, 1–15. https://doi.org/10.1029/2007WR006471

Nyeko-Ogiramoi P, Willems P, Ngirane-Katashaya G (2013) Trend and variability in observed hydrometeorological extremes in the Lake Victoria basin. J Hydrol 489:56–73. https://doi.org/10.1016/j.jhydrol.2013.02.039

Ongoma V, Chen H (2017) Temporal and spatial variability of temperature and precipitation over East Africa from 1951 to 2010. Meteorog Atmos Phys 129:131–144. https://doi.org/10.1007/s00703-016-0462-0

Ongoma V, Chen H, Omony GW (2016) Variability of extreme weather events over the equatorial East Africa, a case study of rainfall in Kenya and Uganda. Theor Appl Climatol 131:295–308. https://doi.org/10.1007/s00704-016-1973-9

Onyutha C (2018) Trends and variability in African long-term precipitation. Stoch Env Res Risk A 32:2721–2739. https://doi.org/10.1007/s00477-018-1587-0

Onyutha C (2017) On rigorous drought assessment using daily time scale: non-stationary frequency analyses, revisited concepts, and a new method to yield non-parametric indices. Hydrology 4(48):1–43. https://doi.org/10.3390/hydrology4040048

Onyutha C (2016a) Geospatial trends and decadal anomalies in extreme rainfall over Uganda, East Africa. Adv Meteorol 2016:1–15. https://doi.org/10.1155/2016/6935912

Onyutha C (2016b) Statistical analyses of potential evapotranspiration changes over the period 1930-2012 in the Nile River riparian countries. Agric For Meteorol 226–227:80–95. https://doi.org/10.1016/j.agrformet.2016.05.015

Onyutha C (2016c) Identification of sub-trends from hydro-meteorological series. Stoch Env Res Risk A 30:189–205. https://doi.org/10.1007/s00477-015-1070-0

Onyutha C (2016d) Statistical uncertainty in hydrometeorological trend analyses. Adv Meteorol 2016:27–26. https://doi.org/10.1155/2016/8701617

Onyutha C, Acayo G, Nyende J (2020) Analyses of precipitation and evapotranspiration changes across the Lake Kyoga Basin in East Africa. Water 12:1–23. https://doi.org/10.3390/w12041134

Onyutha C, Willems P (2017a) Influence of spatial and temporal scales on statistical analyses of rainfall variability in the River Nile basin. Dynamics of Atmospheres and Oceans 77:26–42. https://doi.org/10.1016/j.dynatmoce.2016.10.008

Onyutha C, Willems P (2017b) Space-time variability of extreme rainfall in the River Nile basin. Int J Climatol 37(14):4915–4924. https://doi.org/10.1002/joc.5132

Onyutha C, Willems P (2015) Spatial and temporal variability of rainfall in the Nile Basin. Hydrol Earth Syst Sci 19:2227–2246. https://doi.org/10.5194/hess-19-2227-2015

Owoyesigire B, Mpairwe D, Ericksen P, Peden D (2016) Trends in variability and extremes of rainfall and temperature in the cattle corridor of Uganda. Uganda Journal of Agricultural Sciences 17:231–244. https://doi.org/10.4314/ujas.v17i2.8

Oxfam (2016) Fresh analysis of the humanitarian capacity in Uganda. Oxfam, Kampala, Uganda

Paca V.H. da M, Espinoza-Dávalos GE, Hessels TM, Moreira DM, Comair GF, Bastiaanssen WGM (2019) The spatial variability of actual evapotranspiration across the Amazon River Basin based on remote sensing products validated with flux towers. Ecol Process 8:1–20. https://doi.org/10.1186/s13717-019-0158-8

Parr D, Wang G, Fu C (2016) Understanding evapotranspiration trends and their driving mechanisms over the NLDAS domain based on numerical experiments using CLM4.5. Journal of Geophysical Research: Atmospheres 121:7729–7745. https://doi.org/10.1002/2015JD024398

Pirnia A, Golshan M, Darabi H, Adamowski J, Rozbeh S (2018) Using the Mann–Kendall test and double mass curve method to explore stream flow changes in response to climate and human activities. Journal of Water and Climate Change 10:725–742. https://doi.org/10.2166/wcc.2018.162

Priestley CHB, Taylor RJ (1972) On the assessment of surface heat flux and evaporation using large-scale parameters. Mon Weather Rev 100:81–92. https://doi.org/10.1175/1520-0493(1972)100<0081:OTAOSH>2.3.CO;2

Reliefweb, 2020a. Uganda food security outlook update [WWW document]. OCHA. URL https://reliefweb.int/report/uganda/uganda-food-security-outlook-update-april-2019 (accessed 6.30.20)

Reliefweb, 2020b. Uganda – floods and landslides [WWW document]. OCHA. URL https://reliefweb.int/report/uganda/uganda-floods-and-landslides-dg-echo-iom-world-vision-office-prime-minister-echo-daily (accessed 12.15.20)

Reliefweb, 2018. Karamoja cut-off as floods wash away Kangole Bridge [WWW document]. OCHA. URL https://reliefweb.int/report/uganda/karamoja-cut-floods-wash-away-kangole-bridge (accessed 12.15.20)
Rohwer C (1931) Evaporation from free water surfaces. USDA Technical Bulletin 271:1–96
Running, S., Mu, Q., Zhao, M., 2017. MOD16A2 MODIS/Terra net evapotranspiration 8-day L4 global 500m SIN grid V006 (data set) [WWW document]. NASA EOSDIS Land Processes DAAC. URL https://doi.org/10.5067/MODIS/MOD16A2.006(accessed12.14.20)
Salas JD, Obeysekera J (2014) Revisiting the concepts of return period and risk for nonstationary hydrologic extreme events. J Hydrol Eng 19:554–568. https://doi.org/10.1061/(ASCE)HE.1943-5584.0000820
Sen PK (1968) Estimates of the regression coefficient based on Kendall's tau. J Am Stat Assoc 63:1379–1389. https://doi.org/10.1080/01621459.1968.10480934
Sheffield J, Goteti G, Wood EF (2006) Development of a 50-year high-resolution global dataset of meteorological forcings for land surface modeling. J Clim 19:3088–3111. https://doi.org/10.1175/JCLI3790.1
Shepard, D., 1968. A two- dimensional interpolation function for irregularly- spaced data, in: Proceedings of the 23rd National Conference. Havard College-Cambridge, Massachusetts, pp. 517–524. https://doi.org/10.1145/800186.810616
Sneyers R (1990) On the statistical analysis of series of observations. In: Technical Note No.143, WMO No. 415. Secretariat of the World Meteorological Organization, Geneva, Switzerland
Spearman C (1904) The proof and measurement of association between two things. Am J Psychol 15:72–101
Ssentongo P, Muwanguzi AJB, Eden U, Sauer T, Bwanga G, Kateregga G, Aribo L, Ojara M, Mugerwa WK, Schiff SJ (2018) Changes in Ugandan climate rainfall at the village and forest level. Sci Rep 8(1):1–19. https://doi.org/10.1038/s41598-018-21427-5
Stampone MD, Hartter J, Chapman C, Ryan SJ (2011) Trends and variability in localized precipitation around Kibale National Park, Uganda, Africa. Research Journal of Environmental and Earth Sciences 3:14–23
Sun L, Baker JCA, Gloor E, Spracklen D, Boesch H, Somkuti P, Maeda E, Buermann W (2019) Seasonal and inter-annual variation of evapotranspiration in Amazonia based on precipitation, river discharge and gravity anomaly data. Front Earth Sci 7:1–9. https://doi.org/10.3389/feart.2019.00032
Tang L, Zhang Y (2018) Considering abrupt change in rainfall for flood season division: a case study of the Zhangjia Zhuang reservoir, based on a new model. Water 10:1–16. https://doi.org/10.3390/w10091152
Tarnavsky E, Grimes D, Maidment R, Black E, Allan RP, Stringer M, Chadwick R, Kayitakire F (2014) Extension of the TAMSAT satellite-based rainfall monitoring over Africa and from 1983 to present. J Appl Meteorol Climatol 53:2805–2822. https://doi.org/10.1175/JAMC-D-14-0016.1
Theil, H., 1950. A rank-invariant method of linear and polynomial regression analysis, in: Nederlandse Akademie van Wetenschappen, Series A, A. Statistical Department of the Mathematisch Centrum, Amsterdam, Netherlands, pp. 386–392
Thiery W, Davin EL, Panitz, Jü H, Demuzere M, Lhermitte S, Van Lipzig N (2015) The impact of the African Great Lakes on the regional climate. J Clim 28:4061–4085. https://doi.org/10.1175/JCLI-D-14-00565.1
Thornthwaite CW (1948) An approach toward a rational classification of climate. Geogr Rev 38:55–94
United Nations (2008) UN disaster assessment and coordination (UNDAC) disaster response preparedness mission. United Nations, Kampala, Uganda
Vido J, Nalevanková P, Valach J, Šustek Z, Tadesse T (2019) Drought analyses of the Horné Po žitavie region (Slovakia) in the period 1966-2013. Adv Meteorol 2019:1–10. https://doi.org/10.1155/2019/3576285
Xu Y, Xu Y, Wang Q (2020) Evolution trends in water levels and their causes in the Taihu Basin. China Hydrological Sciences Journal 65:1–37. https://doi.org/10.1080/02626667.2020.1802026

Affiliations

Ambrose Mubialiwo [1,2] · Cyrus Chelangat [1] · Charles Onyutha [2]

[1] Africa Center of Excellence for Water Management, Addis Ababa University, P.O. Box 1176, Addis Ababa, Ethiopia

[2] Department of Civil and Environmental Engineering, Kyambogo University, P.O. Box 1, Kyambogo, Kampala, Uganda